Structural Engineering and Mechanics, *Vol. 67, No. 2 (2018) 207-217*
DOI: https://doi.org/10.12989/sem.2018.67.2.207

Experimental and numerical investigation of strengthened deficient steel SHS columns under axial compressive loads

Mehdi Shahraki[1a], Mohammad Reza Sohrabi[1b], Gholam Reza Azizyan[1c] and Kambiz Narmashiri[*2]

[1]Department of Civil Engineering, University of Sistan and Baluchestan, Zahedan, Iran
[2]Department of Civil Engineering, Zahedan Branch, Islamic Azad University, Zahedan, Iran

(Received January 19, 2018, Revised April 23, 2018, Accepted April 24, 2018)

Abstract. In past years, numerous problems have vexed engineers with regard to buckling, corrosion, bending, and over-loading in damaged steel structures. This article sets out to investigate the possible effects of carbon fiber reinforced polymer (CFRP) and steel plates for retrofitting deficient steel square hollow section (SHS) columns. The effects of axial loading, stiffness, axial displacement, the position and shape of deficient region on the length of steel SHS columns, and slenderness ratio are examined through a detailed parametric study. A total of 14 specimens was tested for failure under axial compression in a laboratory and simulated using finite element (FE) analysis based on a numerical approach. The results indicate that the application of CFRP sheets and steel plates also caused a reduction in stress in the damaged region and prevented or retarded local deformation around the deficiency. The findings showed that a deficiency leads to reduced load-carrying capacity of steel SHS columns and the retrofitting method is responsible for the increase in the load-bearing capacity of the steel columns. Finally, this research showed that the CFRP performed better than steel plates in compensating the axial force caused by the cross-section reduction due to the problems associated with the use of steel plates, such as in welding, increased weight, thermal stress around the welding location, and the possibility of creating another deficiency by welding.

Keywords: Square Hollow Section (SHS); deficiency; CFRP; steel column; strengthening; steel plate

1. Introduction

Steel square hollow sections (SHS) are among the most commonly used structures Bambach *et al.* (2007). Due to errors in design, weakness and errors in the enforcement of structures, poor details in bending and cutting steel reinforcing and placing of stiffeners, fatigue in steel structures in static and dynamic loading for a long time, problems were created in some of the steel beams and column cross-sections due to certain factors such as corrosion of steel cross-sections, cracks, gaps, their extension in the cross-sections of beams and columns, and the weaknesses in designed structures. They were also built in the past using old standards and were prone to failure due to natural disasters, such as winds and earthquakes. Therefore, the need for improvement and restoration is inevitable in order to tackle the increased dead load and fatigue in the desired structures. In order to achieve this, retrofitting and rehabilitation using fiber-reinforced polymer (FRP) composites in the steel structures has been developed. Further, as special equipment is not required to conduct welding operations, the reduction of fatigue in steel structures, high speed performance, the elimination the problems caused by welding, the removal of the stress concentration, and light weight corners of reinforcement plate have been highlighted during recent years.

FRP composites have numerous advantages compared to steel, the most prominent of which are their high strength-to-weight ratio and optimal corrosion resistance. Chloride in the air causes corrosion and crack propagation in welding. Certain factors, such as humidity, salt concentration, and temperature, can create a corrosive environment for welding. Local heating and cooling during welding can produce a non-uniform distribution of temperature, thus causing high residual tensile stresses around the weld zone and the heat affect zone. It is the main source of tension in the stress corrosion of metal. If the sections put pressure on residual stresses from welding, crack propagation will be the actuator Kusnick *et al.* (2013). Indicated the adverse effect of residual stress on buckling strength, while the flame cut type of residual stress was comparatively less effective. Inward and outward imperfections have opposite effects on the critical stress Song *et al.* (2016). The cover should never be below 100% (minimum distance between impacts) because cracks and fatigue can develop under tension in a non-blasted area Dieng *et al.* (2017). Note that steel plates can also be adhesively bonded; however, bonding is less attractive for steel plates due to their heavy weight and inflexibility. In specific applications such as oil storage tanks and chemical

*Corresponding author, Ph.D.
E-mail: narmashiri@iauzah.ac.ir
[a]Ph.D. Candidate
E-mail: m.shahraki@iauzah.ac.ir
[b]Ph.D.
E-mail: sohrabi@hamoon.usb.ac.ir
[c]Ph.D.
E-mail: g.azizyan@eng.usb.ac.ir

http://www.techno-press.com/journals/sem&subpage=7
ISSN: 1225-4568 (Print), 1598-6217 (Online)

plants, where the risk of fire needs to be minimized, welding must to be avoided while strengthening a structure. As a result, the bonding of FRP laminates becomes a very promising alternative. High-strength steel suffers from significant local strength reduction in the heat-affected zone of welds. That is because bonded FRP laminates offer an ideal strength compensation method. Bambach *et al.* (2009) demonstrated the axial capacity and design of thin-walled steel SHS strengthened with CFRP, by describing 20 experiments on short, axially compressed SHSs that were cold-formed from G450 steel and strengthened with externally bonded CFRP. They concluded that the use of CFRP may double the axial capacity by up to 2 times for the capacity of the steel section alone and may enhance the strength-to-weight ratio by up to 1:5 times, as an outcome of the CFRP providing a harness to the outreach of elastic buckling defections and thus provide a reprieve for local buckling. This restraint provides an increase in the buckling stress of up to 4 compared to that of the steel section alone. Teng *et al.* (2012) checked the strengthening of steel structures with fiber-reinforced polymer composites. They concluded that the use of CFRP fibers sufficiently increases the resistance, yield, ultimate strength, and hardness. These fibers are important factors for shear strength, stretch, and toughness to absorb. The rapture level of continuity for the bending strength of steel beams and the buckling of thin-walled steel buildings is an important issue. To overcome the material parameters, adhesion and compression loads must be examined. Benzaid and Mesbah (2013) presented the results of an experimental study on confined concrete square columns using CFRP sheets. The findings reveal that in slender specimens, the collapse was mostly concentrated in their upper or lower areas, and the greater the slenderness ratio, the smaller the region of the CFRP ruptured. Park and Yoo (2013) investigated the experimental results of axially loaded stub columns of slender steel SHSs strengthened with CFRP sheets. To achieve this purpose, 9 specimens were analyzed in their study and the role of the width-to-thickness ratio (b/t), the number of CFRP plates, and the sheet orientation on the ultimate load-carrying capacity were investigated. The results show that using CFRP layers in slender sections has a significant effect on the delays to local buckling and increased inelastic buckling stress. Park and Yoo (2015) discussed the experimental results of flexural and compression steel members strengthened with CFRP sheets. Throughout the course of this experiment, for short columns it was recognized that the two sides would typically buckle outward and the other two sides would buckle inward. For long columns, the overall buckling was attended.

Some researchers investigated the CFRP strengthening of notched damaged steel and concrete structures. Yurdakul and Avar (2017) investigated the structural repairs of a damaged RC beam-column assembly with CFRP. The results indicated that the application of CFRP sheets strengthened the compressed damaged member by increasing its former capacities. Narmashiri *et al.* (2016) studied the strengthening of the steel hollow pipe section using CFRP wraps. They concluded that the application of CFRP layers increased the load bearing capacity, and they also showed that the use of additional CFRP strips enhanced the strength of the strengthened specimens. Su *et al.* (2016) studied the experimental and theoretical of CFRP-restricted damaged and undamaged square RC columns under cyclic loading. The result of their study shows a strong relationship between the numerical models and experimental specimens. Ding *et al.* (2017) investigated the composite action of notched circular CFT stub columns under axial compression. They attempted to study the roles of different parameters on the mechanical behavior of specimens as well as the composite action between the steel tube and the core concrete. They found out that the theoretical formula suggested determining the ultimate load-bearing capacity of the notched CFT stub columns under compression with application of the composite action between the steel tube and the core concrete.

Fewer research studies have examined the CFRP strengthening of notch-damaged steel beam and columns. Ghaemdoust *et al.* (2016) investigated the structural behavior of deficient steel SHS short columns strengthened by CFRP. Eight deficient specimens were repaired using CFRP sheets. The results indicated that the application of CFRP sheets for strengthening deficient steel short SHS columns could help in significantly recovering the strength lost due to the deficiency. An increment on the load-bearing capacity and a delay in local buckling were also observed. Yousefi *et al.* (2017) studied the effect of CFRP strips on strengthening notched steel beams. They point out that the application of CFRP plates in the deficiency region prevents crack propagation and brittle fractures. Karimian *et al.* (2017) studied the effects of deficiency on reducing axial resistance and the possibility of overcoming weakness on CHS short columns strengthened using CFRP sheets. They considered CFRP layers as leading to reduced stress in the damage region, a higher load-carrying capacity, and the prevention of local buckling around the deficient region. Previous works have focused only on the application of CFRP in strengthening notched damage on short steel columns. In addition, no research appears to have surveyed the use of CFRP sheets and steel plates on retrofitting deficient intermediate and slender steel SHS columns. Considering these aims, the current study investigated the steel SHS columns using two methods: welding steel plates and wrapping by CFRP sheets under axial compression loads. Another objective of the article is to compare strengthening with the consideration of limitations and the advantages of both methods, and removing the shortcomings caused by the deficiency.

2. Materials and methods

2.1 Materials

2.1.1 Steel columns

The section sizes employed for the SHS steel columns test were SHS 40×40×2(mm) and SHS 80×80×2(mm). The length of each steel column was 2500(mm). The boundary conditions of the specimens were designed to provide fixed support using one steel plate and four equal-leg angles that welded the end of the columns. Prior to commencing the study, for investigating effect of the deficiency on the ultimate load-carrying capacity of the columns, seven

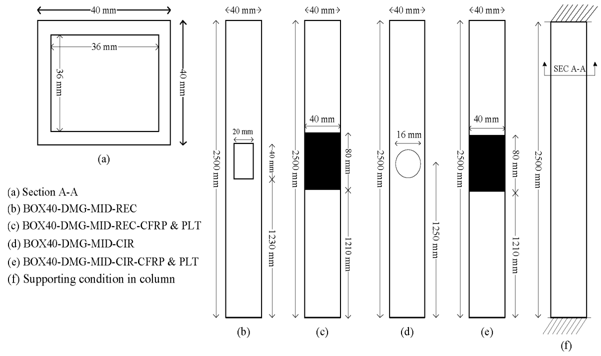

Fig. 1 Measured geometric dimensions of the BOX40

Table 1 Material properties of steel columns

Steel Hollow Section Columns Specifications				Modulus of Elasticity (MPa)	stress (MPa)		Elongation(%)
Specimen Label	Thickness (mm)	Height (mm)	Deficient Cross Sectional Area (mm^2)		Yield stress	Ultimate stress	
BOX40&BOX80	2	2500	800 & 3200	219267	366	398	15.794

Table 2 Material properties of carbon fiber. (Sikawrap-230C 2006)

Tensile strength (MPa)	Tensile E-Modulus (MPa)	Ultimate strain (%)	Thickness (mm)	Width (mm)
4300	238000	1.8	0.131	500

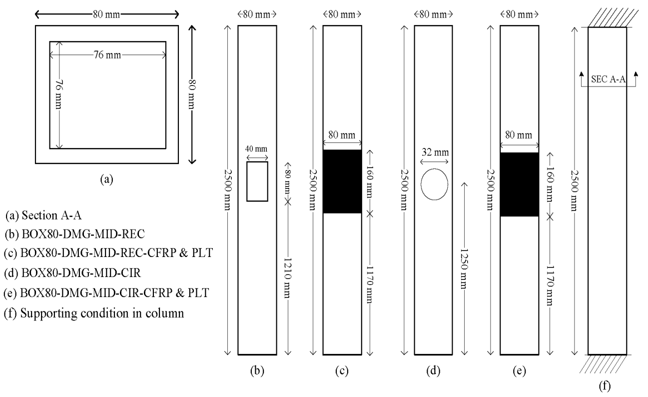

Fig. 2 Measured geometric dimensions of the BOX80

80×80×2(mm) columns with a slenderness ratio ($\lambda = k \times l / r$) equal to 33.5 and seven 40×40×2(mm) specimens with $\lambda = 80$ were used. The effective length factor (k) was assumed to be 0.5. After comparing the effect of position, cross-section, and shape of damage, two kinds of defects were identified: (a) a rectangular deficient region with a specified dimension in the middle of the length column, and (b) a circular deficient region with the same area and position as the rectangular deficient region. In the end, two columns were improved without retrofitting and the other columns were strengthened using CFRP sheets and steel plates. The layer cover of CFRP in the deficiency area can be twice as much as that of the vertical height of the defects. The height of the steel plate is also similar to that of the CFRP fibers. The material properties and information, regarding to the SHS steel columns and also the results of steel plate tensile test

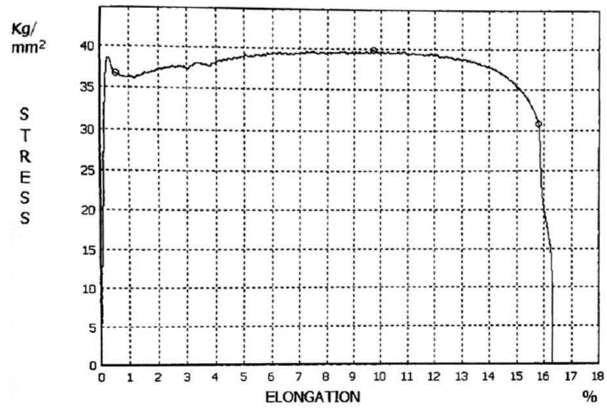

Fig. 3 Stress-strain curve for steel material

are shown in Table 1. Figs. 1 and 2 present the information on the defects created and the cross-sectional dimensions in specimens. Furthermore, some terms are used for the specimens: BOX=Steel SHS Column; DMG=Deficient; MID=Middle; REC=Rectangular Deficient; CIR=Circular Deficient; PLT=Steel Plate. According to the standards of ASTMA370, AASHTOT299. Fig. 3 illustrates the tested stress-strain curves.

2.1.2 CFRP

The CFRP used in this study is unidirectional Sikawrap 230-C (Sikawrap-230C 2006). The properties of the carbon fiber supplied by the manufacturer are indexed in Table 2.

2.1.3 Adhesive

Adhesive supplies the power transmission path between the steel and composite materials. Adhesive causes the identical performance of the composite and columns. The CFRP sheets are attached to the steel columns using Sikadur-330 epoxy (Sikadur-330 2012). The epoxy used by the supplier of CFRP is the proposed product shown in Table 3.

2.2 Research methods

2.2.1 Experimental specimens preparation

A total of 14 specimens were prepared the defects in columns created by CNC machine. Then, the specimens were sandblasted to remove all external infects. The loose steel particles and grease were removed by using acetone and cotton. Subsequently, the CFRP sheets were cut to the appropriate dimensions by a cutter and were wrapped around the defective areas on the steel SHS columns by using four layers (two longitudinal and two transverse) according to the manufacturer's instruction regarding the overlap conditions and adhesive geometrical mix design. The steel plates were welded to the defective regions. Finally, the specimens were placed in the laboratory at room temperature for at least one week before testing. Fig. 4 shows the preparation procedures for the steel columns.

The experimental program was conducted in the laboratory of the Civil Engineering Department at the Islamic Azad University. Specimens were loaded under a monotonic uni-axial compression load up to failure. The

Fig. 4 Preparation of CFRP strengthened specimens

Table 3 Properties of the adhesive Sikadur-330 (2012)

Tensile strength (*MPa*)	Flexural E-Modulus (*MPa*)	Tensile E-Modulus (*MPa*)	Elongation at break (*%*)
30	3800	4500	0.9

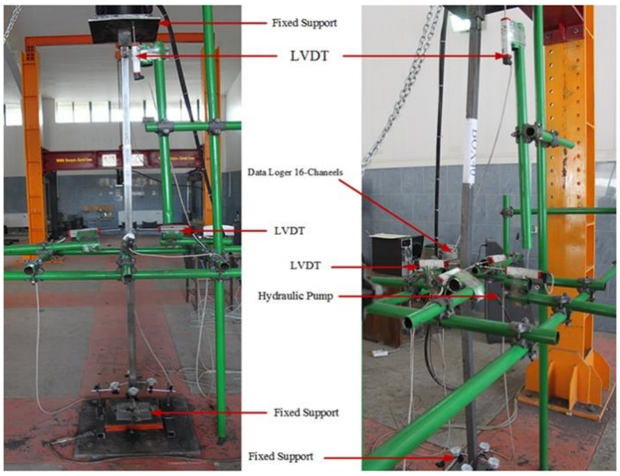

Fig. 5 Test Setup for local-overall buckling tests

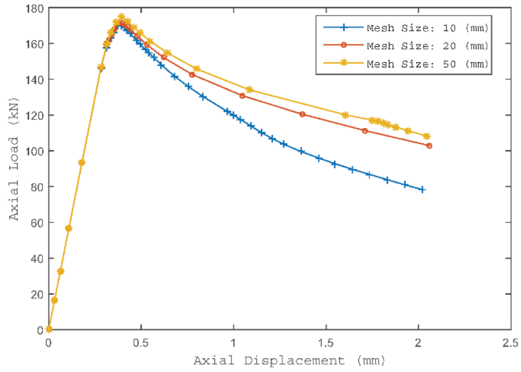

Fig. 6 Mesh size studied

load was applied using a hydraulic universal testing machine with a vertical load capacity of 1000 (*kN*). The load-carrying capacity (P_{cr}) and maximum axial displacement (δmax) were measured by linear variable differential transformer (LVDT) connected to the top of the columns. The load cell and LVDT were connected to a 16-channel data logger to save and record the data. Fig. 5 shows the test setup. The test was conducted until either the specimen failed due to a fracture of the steel SHS or the loading device was stopped.

2.2.2 FE simulation

In order to perform a FE model analysis for the CFRP strengthened steel SHS columns, Abaqus ver. 6.14.1 was used for this study. Then for the analysis, the local buckling behaviors of an SHS steel column, CFRP, steel plate, and adhesive were studied by employing the 3D-8R node HEX element. The static risk analysis method was utilized in the simulation to observe the plastic zone buckling post buckling. The material properties of the steel plates and the CFRP sheets, the yield, and the ultimate strength values of the steel SHS columns were equal to the values obtained from the coupon test results. Poisson's ratio was also 0.3. An adequate modeling of the end support conditions was used by fix end conditions, so preventing all their local buckling and rotations at end part of specimens Park *et al.* (2013). Tie Method was applied to connect the adhesive and CFRP to the steel column and to generate the desire surface interaction. The linear and nonlinear properties of materials were defined. The CFRP strips material properties were defined as linear and orthotropic, because CFRP materials have shown linear properties and are unidirectional. The other materials were determined as nonlinear and isotropic properties Narmashiri *et al.* (2011). Selected of 10 (*mm*) meshing size compared to different mesh size studied. Fig. 6 presents the procedure use to select the mesh size. In this section, we first verify the software and the accuracy of the

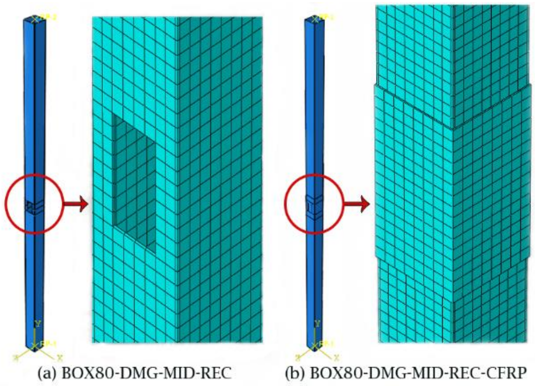

Fig. 7 The schematic of finite element modeling

test results conducted by Park *et al.* (2013). Fig. 7 shows the schematic of finite element modeling. The results obtained from computing the difference in load and axial displacement for the specimens is minimal in both the experimental and analytically modes of the software, as presented in Fig. 8.

3. Results and discussions

3.1 Load carrying capacity and overall observations

Bambach *et al.* (2009) investigated the design and

Table 4 Summery of test and FEM results in BOX40

Specimen label	Item	Results		Value of gain or loss		% gain or loss		Errors	
		Test	FEM	Test	FEM	Test	FEM	$P(Test/FEM)$	$K(Test/FEM)$
BOX40	maximum load(*kN*)	97.86	95.48	Control	Control	Control	Control	1.02	-
BOX40	Stiffness(*kN*/*mm*)	22.87	22.88	Control	Control	Control	Control	-	0.99
BOX40-DMG-MID-REC	maximum load(*kN*)	66.00	66.02	−31.86	−29.46	−48.27	−44.62	0.99	-
BOX40-DMG-MID-REC	Stiffness(*kN*/*mm*)	21.15	21.93	−1.72	−0.95	−8.13	−4.33	-	0.96
BOX40-DMG-MID-REC-CFRP	maximum load(*kN*)	72.54	78.03	6.54	12.01	9.01	15.39	0.93	-
BOX40-DMG-MID-REC-CFRP	Stiffness(*kN*/*mm*)	21.98	26.01	0.83	4.08	3.92	18.60	-	0.85
BOX40-DMG-MID-REC-PLT	maximum load(*kN*)	68.58	64.03	2.58	−1.99	3.76	3.01	1.07	-
BOX40-DMG-MID-REC-PLT	Stiffness(*kN*/*mm*)	22.86	22.07	1.71	0.14	7.48	0.63	-	1.04
BOX40-DMG-MID-CIR	maximum load(*kN*)	54.00	53.50	−43.86	−41.98	−44.81	−43.96	1.01	-
BOX40-DMG-MID-CIR	Stiffness(*kN*/*mm*)	20.61	21.83	−2.26	−1.05	−9.88	−4.59	-	0.94
BOX40-DMG-MID-CIR-CFRP	maximum load(*kN*)	64.98	66.74	10.98	13.25	16.89	1.92	0.97	-
BOX40-DMG-MID-CIR-CFRP	Stiffness(*kN*/*mm*)	18.88	21.39	−1.73	0.43	−8.39	1.97	-	0.88
BOX40-DMG-MID-CIR-PLT	maximum load(*kN*)	48.90	49.19	5.10	4.30	9.44	8.04	0.99	-
BOX40-DMG-MID-CIR-PLT	Stiffness(*kN*/*mm*)	20.37	25.89	−0.22	4.06	−1.14	15.68	-	0.79
Mean								0.9999	0.9224
St.dev								0.0016	0.0124

capacity of 20 steel SHSs strengthened with CFRP and found out which CFRP doubles the cross-section axial capacity and increases the resistance-to-weight ratio by one-and-a-half times. Bambach *et al.* (2009) examined the axial capacity and crushing behavior of metal fiber square tubes of steel, stainless steel, and aluminum strengthened with CFRP. Fracture models, stress-strain behavior, and ultimate bearing capacity of short steel square columns retrofitted with CFRP were studied by Sivasankar *et al.* (2013). The paper investigates the effects of shape and position on the deficiency by using CFRP and steel plates to study the load bearing capacity of the steel SHS columns. The results obtained from the preliminary analysis of (P_{cr}) are shown in Tables 4 and 5.

3.2 Behavior of columns in group #1

Group #1 included seven columns, two of which were of the normal type of BOX40, and the rest had artificial defects, strengthened using CFRP and steel plates. Fig. 9 and Table 4 provide the maximum load and stiffness of the columns.

In Table 4, the results of the maximum load obtained from the tests and the FEM analysis are summarized. Also, the results show a good correlation between the test and the FEM results as shown in Table 4. The mean and standard deviation of the $P(Test/Fem)$ ratio were 0.9999 and 0.0016 respectively. Stiffness is defined as shown in Eq. (1) and the definition of stiffness is shown in Fig.10. In the work of Park *et al.* (2013), $0.75P_{\max}$ is the axial load when the load attains 75% of the maximum load in the pre-peak stage and $P_{\max}$ is the maximum load point. Also, P_k is the load for the cross-line point lines (1) and (2) in Fig. 10.

$$K_i = \left(P_k / \delta_y\right) \tag{1}$$

The test stiffness values K_{Test} were quite close to the stiffness values K_{Fem} provided by FEM analysis, as shown in Table 4. The mean and standard deviation of the $K(Test/Fem)$ ratio were 0.9224 and 0.0124 respectively. The results of Table 4 showed that creating a rectangular deficient region at the middle of the square column is responsible for the decrease in the maximum ultimate load by 48.27% and in stiffness by 8.13%. The use of CFRP is responsible for the 9.1% increase in the maximum tolerable load compared to the control specimen. At the same time, using a steel plate for retrofitting causes a 3.76% increase in the maximum load-bearing capacity. The results obtained from Table 4, In the BOX40 columns, creating a rectangular deficient region decreases the maximum load-carrying capacity by 31.86% and stiffness by 1.72%. Using CFRP is responsible for the 6.54% increase in the maximum load-carrying capacity compared to BOX40 with a rectangular defect in the middle of the column. At the same time, using steel plate for strengthening causes a 2.58% increase in the maximum load. The load-carrying capacity in columns with

Table 5 Summery of test and FEM results in BOX80

Specimen label	Item	Results		Value of gain or loss		% gain or loss		Errors	
		Test	FEM	Test	FEM	Test	FEM	*P*(*Test*/*FEM*)	*K*(*Test*/*FEM*)
BOX80	maximum load(*kN*)	215.82	208.71	Control	Control	Control	Control	1.00	-
BOX80	Stiffness(*kN*/*mm*)	46.01	45.76	Control	Control	Control	Control	-	1.03
BOX80-DMG-MID-REC	maximum load(*kN*)	172.26	169.92	−43.56	−38.78	−25.28	−22.82	1.01	-
BOX80-DMG-MID-REC	Stiffness(*kN*/*mm*)	44.97	43.23	−1.04	−2.53	−2.31	−5.85	-	1.04
BOX80-DMG-MID-REC-CFRP	maximum load(*kN*)	218.58	209.06	46.30	39.14	26.88	23.03	1.05	-
BOX80-DMG-MID-REC-CFRP	Stiffness(*kN*/*mm*)	56.76	53.06	11.79	9.83	26.21	22.73	-	1.07
BOX80-DMG-MID-REC-PLT	maximum load(*kN*)	207.60	208.21	35.34	38.29	20.51	22.53	0.99	-
BOX80-DMG-MID-REC-PLT	Stiffness(*kN*/*mm*)	45.93	44.90	10.96	1.67	2.13	3.86	-	1.00
BOX80-DMG-MID-CIR	maximum load(*kN*)	143.80	143.13	−72.02	−65.58	−50.08	−45.81	1.00	-
BOX80-DMG-MID-CIR	Stiffness(*kN*/*mm*)	39.07	34.86	−6.94	−10.90	−17.76	−31.26	-	1.12
BOX80-DMG-MID-CIR-CFRP	maximum load(*kN*)	217.62	209.32	73.82	66.19	51.33	46.24	1.04	-
BOX80-DMG-MID-CIR-CFRP	Stiffness(*kN*/*mm*)	45.71	46.61	6.64	11.75	16.99	33.70	-	0.98
BOX80-DMG-MID-CIR-PLT	maximum load(*kN*)	141.00	141.51	−2.80	−1.62	1.98	1.14	0.99	-
BOX80-DMG-MID-CIR-PLT	Stiffness(*kN*/*mm*)	53.20	51.73	14.13	16.86	36.16	48.38	-	1.02
Mean								1.0177	1.0352
St.dev								0.0004	0.0019

a circular deficient region in the middle caused a decrease of 44.81% in the maximum axial force compared to the control sample. The use of CFRP and a steel plate is responsible for increases load bearing capacity of 16.89% and 9.44%, respectively.

As can be seen from the Table 4, In the BOX40 columns, creating a circular deficient region decreases the maximum load-carrying capacity by 43.86% and stiffness by 2.26%. Using CFRP is responsible for the 10.98% increase in the ultimate load compared to BOX40 with the same deficiency in the specimen. At the same time, using a steel plate for strengthening causes a 5.1% increase in the maximum load. The results indicated that the most critical mode was a circular deficient region in the middle of the column, which proves that since the selected columns are slender, they tend to buckle. The 38% difference of the maximum of the axial force proves this. For the test results, the stiffness of the SHS columns damage was an increase or decrease of 8.1, -1.73 for the rectangular/circular deficient region when using CFRP sheets, and 1.71, -0.215 using a steel plate. The data in Table 4 reveals that using CFRP gives a better performance than the steel plate, and the response rate is 5.4% at BOX40 with a rectangular deficient region and 27.74% at BOX40 with circular damage in the middle of the length of the columns. Fig. 11 shows the stress distribution around the rectangular deficient region at the middle of the column due to the axial load applied by the Jack in the laboratory. The overall buckling was observable due to the low width and thickness (*b*/*t*).

Fig. 12 shows local and overall buckling around the region of deficiency on the steel column with a circular defect in the middle of the SHS. Fig. 13 also shows the typical overall buckling in BOX40 with a rectangular/circular deficient region, using CFRP fibers.

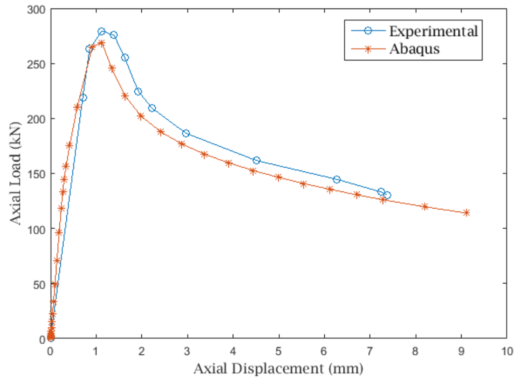

(a) BT100-0P

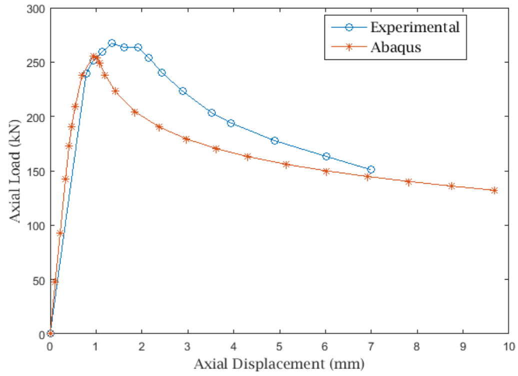

(b) BT80-1P

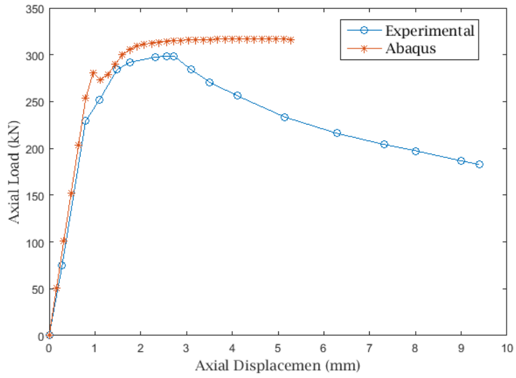

(c) BT80-3P

Fig. 8 Comparison of Load-Displacement curve results of FEM with experimental data of Park *et al.* (2013)

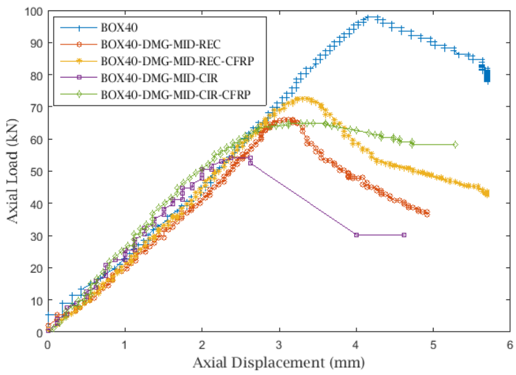

(a) Experimental specimens of BOX40 strengthening with CFRP

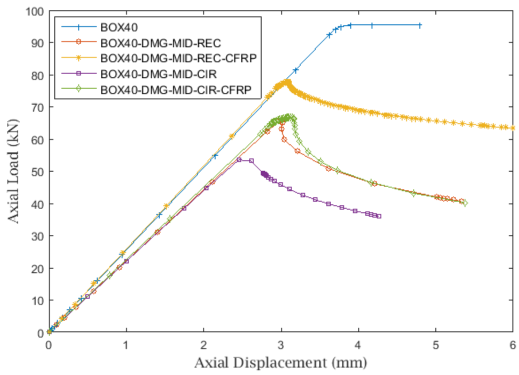

(b) Simulated specimens of BOX40 strengthening with CFRP

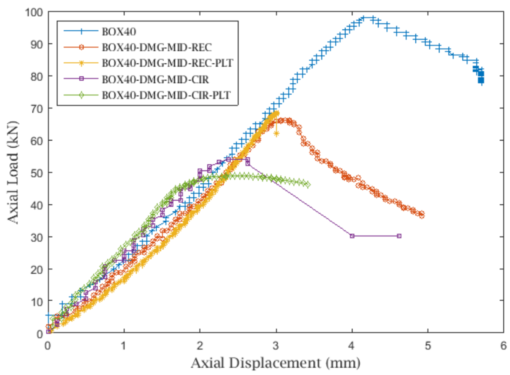

(c) Experimental specimens of BOX40 strengthening with steel plate

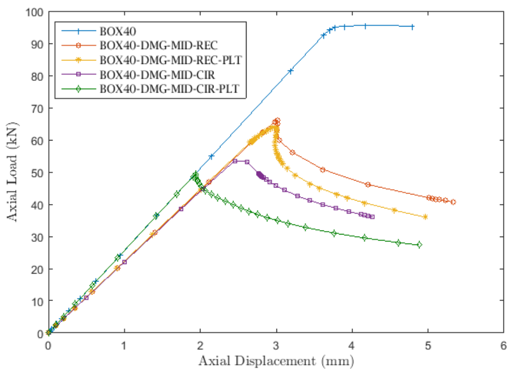

(d) Simulated specimens of BOX40 strengthening with steel plate

Fig. 9 Comparison of test and simulated load displacement curves in BOX40 specimens

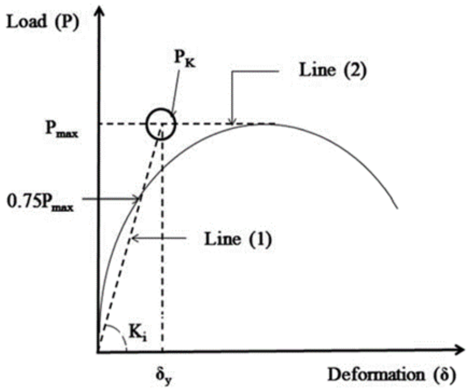

Fig. 10 Definition of stiffness Park *et al.* (2013)

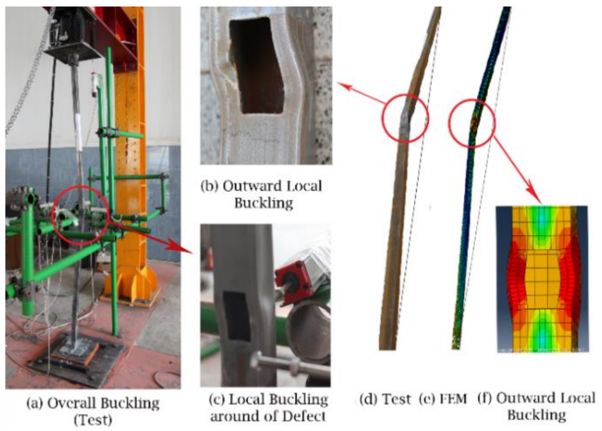

Fig. 11 Comparison of failure modes from the interactive buckling test and FE modelling in BOX40-DMG-MID-REC

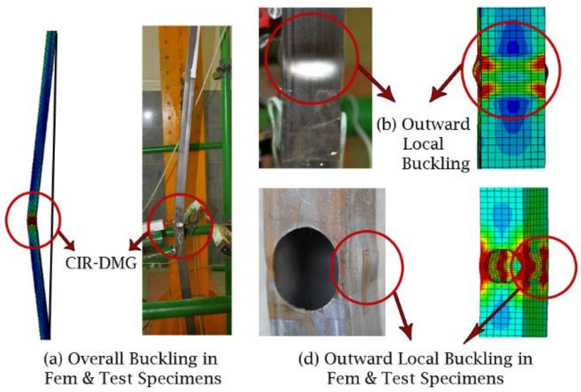

Fig. 12 Comparison of failure modes from the interactive buckling test and FEM modeling in BOX40-DMG-MID-CIR

Therefore, the figures above show that CFRP sheets can delay local buckling by having a confining effect on the outward local buckling sides, and they can improve the axial load capacity of steel SHS columns. Fig. 14 shows the overall buckling in BOX40 with rectangular damage using a steel plate.

3.3 Behavior of columns in group #2

Group #2 included seven columns, two of which were of

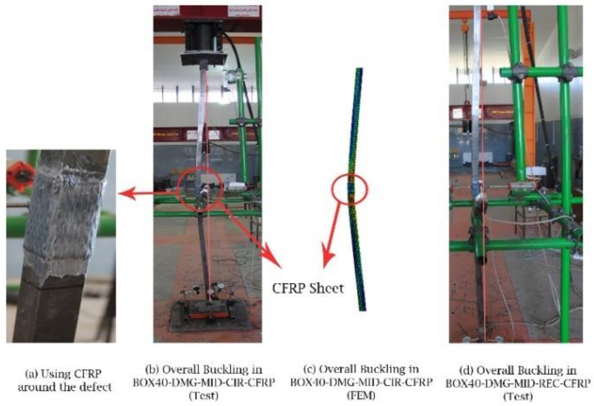

Fig. 13 Typical the overall buckling test and FEM modeling in BOX40-DMG-MID-REC & CIR using CFRP sheets

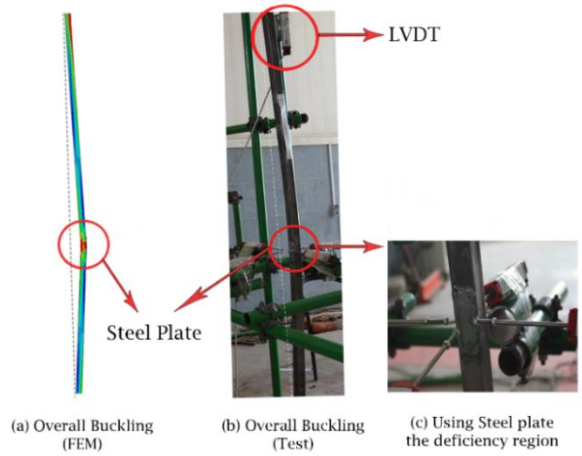

Fig. 14 Comparison of overall buckling the test and FEM modeling in BOX40-DMG-MID-REC using steel plate

the normal type of BOX80, and the rest had artificial defects, strengthened using CFRP and steel plates. Fig. 15 and Table 5 provide the maximum load and stiffness of the columns.

The Table 5 illustrates the results of load-carrying capacity obtained from the tests and the FEM analysis. The results show a good correlation between the test results and the FEM results. The maximum load values P_{Test} obtained by the test were quite similar to the maximum load values P_{Fem} provided by the FEM analysis, as shown in Table 5.

The mean and standard deviation of the $P(Test/Fem)$ ratio were 1.01774 and 0.00042 respectively. The test stiffness values K_{Test} were quite close to the stiffness values K_{Fem} provided by the FEM analysis, as shown in Table 5. The mean and standard deviation of the $K(Test/Fem)$ ratio were 1.0352 and 0.0019 respectively. The results of Table 5 indicate that a slight difference is found between the experimental and numerical (Abaqus) results in terms of maximum load-carrying capacity and column stiffness. The rectangular deficient region at the middle of the column is responsible for 25.28% tolerable force, while the circular deficient region in the middle of the column causes a 50.08% decline in tolerable force compared to the control sample. It can be seen from the data in Table 5 that, In the BOX80 columns, creating a rectangular deficient region in

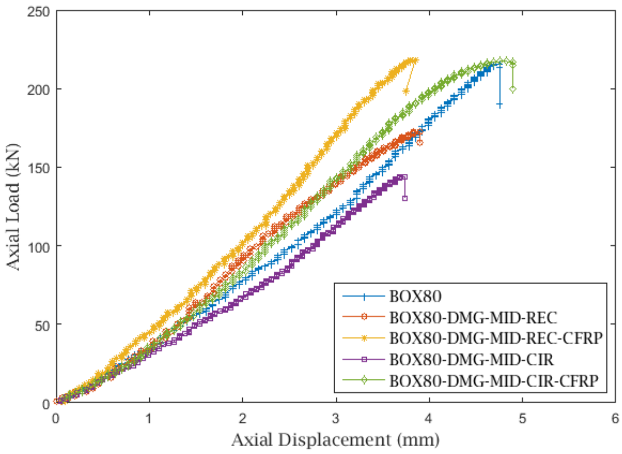

(a) Experimental specimens of BOX80 strengthening with CFRP

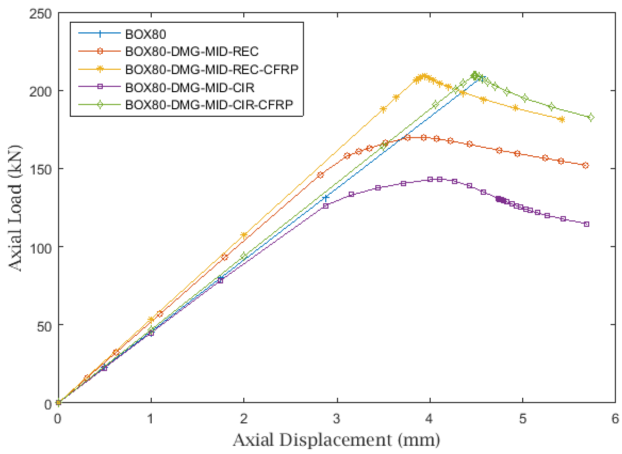

(b) Simulated specimens of BOX80 strengthening with CFRP

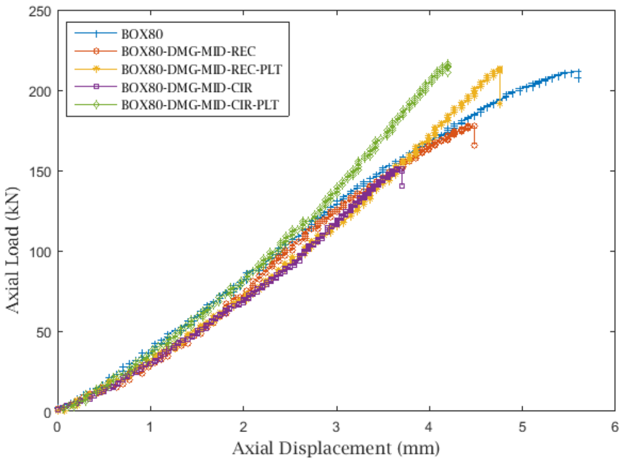

(c) Experimental specimens of BOX80 strengthening with steel plate

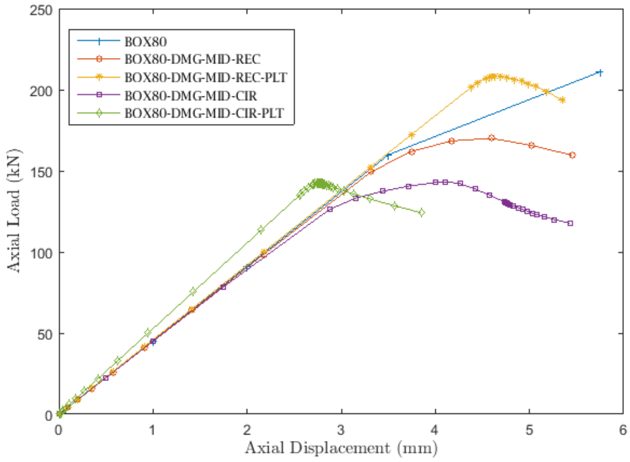

(d) Simulated specimens of BOX80 strengthening with steel plate

Fig. 15 Comparison of test and simulated local displacement curves in BOX80 specimens

the middle is responsible for a 25.28% decrease in the load carrying capacity and a circular one in the middle of the thin-walled steel column by 50.08%. A steel SHS column with a rectangular deficient region that is retrofitted by CFRP sees an increase of 26.88% in the axial load capacity. There is also an increase of 20.51% in the maximum load upon using a steel plate.

A thin-walled steel column with a rectangular deficient region in the middle of the length of the column retrofitted by CFRP causes an increase of 26.88% in the axial load-carrying capacity. If the steel plate is welded, the reduction is reported to be 20.51% at the deficient location compared to the control specimen. Using CFRP and steel plates is responsible for increases of 51.33% and 1.98% in the load-carrying capacity of the columns with a circular deficient region in the middle compared to the column without retrofitting, respectively. Table 5 illustrates that using CFRP sheets provides better performance than the steel plate, and the response rate is 54.34% at BOX80 with a circular deficiency in middle of the column. It is apparent from this table that the SHS column with a circular deficient shape is more critical than the column with rectangular damage. In order to, for the test results, the load bearing capacity of the circular deficient was decrease 19.79% rather than the rectangular deficient in middle length of columns. As expected, the increase in the width-to-thickness: (*b*/*t*) ratio of BOX80 compared to BOX40 leads to a higher tendency of local buckling at the cross-section (see Figs. 16-18). It is apparent from Table 5 that, no significant difference was found in terms of the maximum load in BOX80 retrofitted with CFRP and steel plates. Fig. 16 shows local buckling and deformation around the rectangular and circular deficient region and stress concentration around BOX80. Fig. 17 shows the BOX80 retrofitted by CFRP layers with a rectangular deficient region. As can be seen, using CFRP prevents deformation around the deficient region and the deformation caused by local buckling.

Fig. 18 also shows overall-local buckling above the CFRP sheet. Fig. 19 shows the use of a steel plate to prevent local deformation around the circular deficient region in the steel column. As shown in Figs. 16-19, CFRP and steel plates could confine local buckling, and the CFRP layers are effective in enclosing the deformation around the deficiency locations.

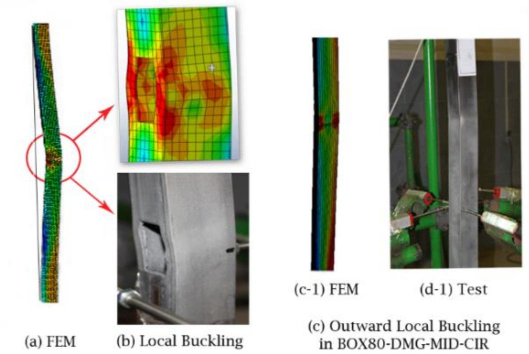

Fig. 16 Typical failure mode in BOX80-DMG-MID-REC & BOX80-DMG-MID-CIR

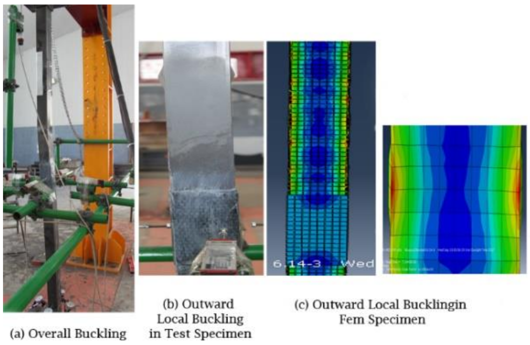

Fig. 17 Comparison the outward local buckling test and FEM in BOX80-DMG-MID-REC-CFRP

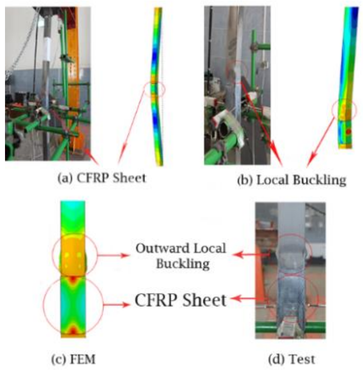

Fig. 18 Comparison of Overall-Local buckling test and FEM modeling in BOX80-DMG-MID-CIR-CFRP

3.4 Failure modes

All the specimens were tested under axial compression until failure. The typical failure modes of BOX40 specimens are shown in Figs. 11 and 12. For the non-strengthening specimens, both inward and outward local buckling was observed in the deformed specimens, whereas for retrofitting SHS with CFRP, local buckling was prevented by the CFRP sheets. Finally, for example, Figs. 13-14 show that the CFRP layers and steel plates played an appropriate role in retarding or overcoming the local buckling in the BOX40 columns. The BOX80 columns were inclined to greater local buckling prior to overall buckling due to the increase in (b/t). This is shown in Figs. 16-19. In all of the figures, the deformation obtained from the FEM analyses agrees reasonably well with the experimental observations.

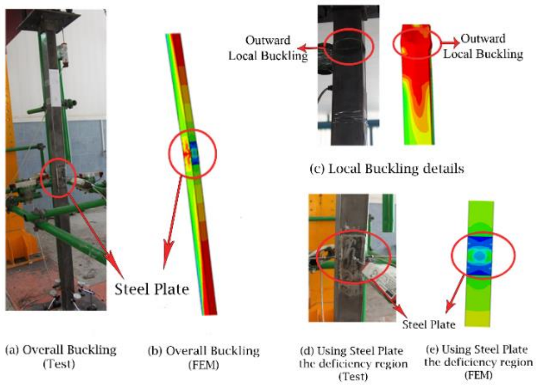

Fig. 19 Typical the Overall-local buckling test and FEM modeling in BOX80-DMG-MID-CIR-PLT

3.5 Influence of slenderness

For the columns with lower slenderness, the cross-section of the columns is under compression. However, there is a region on the mid-height cross-section under tensile in the longitudinal direction for the columns with higher slenderness. Increasing the slenderness ratio results in a decrease in the strengthening effect of stress distribution around the damaged location, in the load-carrying capacity of the specimens.

4. Conclusions

In this article, 14 specimens of SHS steel columns with two types of damage were strengthened using CFRP sheets and steel plates. The effects of different parameters on the response of the repaired columns, including the effect of the position and cross-section of the defect in the length of the columns, the maximum load and stiffness values, and the strengthening effect of the CFRP sheets and steel plates were studied. The FEM program Abaqus ver. 6.14.1 was used for this study. The research findings lead to the following conclusions: (1) The finite element simulation results of the deformed mode of the steel columns agree well with the experimental results. The stress distributions of different specimens and failure modes have been analyzed, and the computed results show good agreement with the experimental results. (2) This study confirms that retrofitting methods are effective in expanding the local and overall buckling, decreasing stress around the damage location, and increasing the ductility. One unanticipated finding is that the BOX80 columns are inclined to greater local buckling prior to overall buckling due to the increase in (b/t). (3) In BOX80 the applied CFRP layers were able to regain the strength to that of the undamaged strength of the section. (4) The stiffness caused by the maximum load-carrying capacity and maximum vertical were also investigated. The mean and standard deviation were calculated for both the lab and numerical modes. The results showed that the stiffness declined as a result of creating a deficient region. (5) This research showed that CFRP sheets perform better than steel plate in compensating the axial force caused by the cross-section reduction due to the problems associated with the use of steel plates, such as welding, increased weight, thermal stress around welding location, and the possibility of creating another deficiency by welding. (6) The current study found that the CFRP strengthening is useful for overcoming the weakness and improving the performance of deficient intermediate and slender steel SHS columns.

Acknowledgments

This study was financially supported by Islamic Azad University, Zahedan, Iran. The authors would like to thank everyone involved for their support.

References

Bambach, M., Elchalakani, M. and Zhao, X.L. (2009), "Composite steel-CFRP SHS tubes under axial impact", *Thin-Wall. Struct.*, **87**(3), 282-292.

Bambach, M., Jama, H. and Elchalakani, M. (2009), "Axial capacity and design of thin-walled steel SHS strengthened with CFRP", *Thin-Wall. Struct.*, **47**(10), 1112-1121.

Bambach, M.R. and Elchalakani, M. (2007), "Plastic mechanism analysis of steel SHS strengthened with CFRP under large axial deformation", *Thin-Wall. Struct.*, **45**(2), 159-170.

Benzaid, R. and Mesbah, H.A. (2013), "Strength model for square concrete columns confined by external CFRP sheets", *Struct. Eng. Mech.*, **46**(1), 111-135.

Dieng, L., Amine, D., Falaise, Y. and Chataigner, S. (2017), "Parametric study of the finite element modeling of shot peening on welded joints", *Constr. Steel Res.*, **130**, 234-247.

Ding, F., Wen, B., Liu, X. and Wang, H. (2017), "Composite action of notched circular CFT stub columns under axial compression", *Steel Compos. Struct.*, **24**(3), 309-322.

Ghaemdoust, M., Narmashiri, K. and Yousefi, O. (2016), "Structural behaviors of deficient steel SHS short columns strengthened using CFRP", *Constr. Build. Mater.*, **126**, 1002-1011.

Karimian, M., Narmashiri, K., Shahraki, M. and Yousefi, O. (2017), "Structural behaviors of deficient steel CHS short columns strengthened using CFRP", *J. Constr. Steel Res.*, **138**, 555-564.

Kusnick, J., Benson, M. and Lyons, S. (2013), *Finite Element Analysis of Weld Residual Stresses in Austenitic Stainless Steel Dry Cask Storage System Canisters*, Technical Letter Report, ML13330A512.

Narmashiri, K. and Jumaat, M.Z. (2011), "Reinforced steel I-beams: A comparison between 2D and 3D simulation", *Simulat. Model. Pract. Theor.*, **19**(1), 564-585.

Narmashiri, K. and Mehramiz, G. (2016), "Strengthening of steel hollow pipe sections subjected to transverse loads using CFRP", *Struct. Eng. Mech.*, **60**(1), 163-173.

Narmashiri, K., Jumaat, M.Z. and Ramli Sulong, N.H. (2010), "Shear strengthening of steel I-beams by using CFRP strips", *Sci. Res. Ess.*, **5**(16), 2155-22168.

Park, J.W. and Yoo, J.H. (2013), "Axial loading tests and load capacity prediction of slender SHS stub columns strengthened with carbon fiber reinforced polymers", *Steel Compos. Struct.*, **15**(2), 131-150.

Park, J.W. and Yoo, J.H. (2015), "Flexural and compression behavior for steel structures strengthened with carbon fiber reinforced polymers (CFRPs) sheet", *Steel Compos. Struct.*, **19**(2), 441-465.

Park, J.W., Yeom, H.J. and Yoo, J.H. (2013), "Axial loading test and FEM analysis of slender square hollow section (SHS) stub columns strengthened with carbon fiber reinforced polymers", *Int. J. Steel Struct.*, **13**(4), 731-743.

Sikadur-330 (2012), *Product Data Sheet*, Edition 21/02/2012, Westmead, South Africa.

Sikawrap-230C (2006), *Product Data Sheet*, Edition 13/06/2006, Adliya, Kingdom of Bahrain.

Sivasankar, S., Thilakramjith, T. and Sundarraja, M.C. (2013), "Axial behavior of CFRP jacketed HSS tubular members an experimental investigation", *Int. J. Earth Sci. Eng.*, 1729-1737.

Song, Y.C., Wang, R.P. and Li, J. (2016), "Local and post-local buckling behavior of welded steel shapes in partially encased composite columns", *Thin-Wall. Struct.*, **108**, 93-108.

Su, Li., Li, X. and Wang, Y. (2016), "Experimental study and modelling of CFRP-confined damaged and undamaged square RC columns under cyclic loading", *Steel Compos. Struct.*, **21**(2), 411-427.

Teng, J.G., Yu, T. and Fernando, D. (2012), "Strengthening of steel structures with fiber-reinforced polymer composites", *J. Constr. Steel Res.*, **78**, 131-143.

Yousefi, O., Narmashiri, K. and Ghaemdoust, M.R. (2017), "Structural behaviors of notched steel beams strengthened using CFRP strips", *Steel Compos. Struct.*, **25**(1), 35-43.

Yuan, H.X., Wang, Y.Q., Gardner, L. and Shi, Y.J. (2014), "Local overall interactive buckling of welded stainless steel box section compression members", *Eng. Struct.*, **67**, 62-76.

Yurdakul, O. and Avar, O. (2017), "Structural repairing of damaged reinforced concrete beam-column assemblies with CFRPs", *Struct. Eng. Mech.*, **54**(3), 521-543.

CC